Bifurcation and chaos in coupled ratchets exhibiting synchronized dynamics

U. E. Vincent,[1,2] A. Kenfack,[3,4,*] A. N. Njah,[1] and O. Akinlade[1]
[1]*Department of Physics, College of Natural Sciences, University of Agriculture, Abeokuta, Nigeria*
[2]*Department of Physics and Solar Energy, Bowen University, Iwo, Nigeria*
[3]*The University of Dschang, Faculty of Science, Physics Department, P.O. Box 67, Dschang, Cameroon*
[4]*Max Planck Institute for the Physics of Complex Systems, Nöthnitzer Strasse 38, 01187 Dresden, Germany*
(Received 23 May 2005; revised manuscript received 15 August 2005; published 17 November 2005)

The bifurcation and chaotic behavior of unidirectionally coupled deterministic ratchets is studied as a function of the driving force amplitude (a) and frequency (ω). A classification of the various types of bifurcations likely to be encountered in this system was done by examining the stability of the steady state in linear response as well as constructing a two-parameter phase diagram in the (a-ω) plane. Numerical explorations revealed varieties of bifurcation sequences including quasiperiodic route to chaos. Besides, the familiar period-doubling and crises route to chaos exhibited by the one-dimensional ratchet were also found. In addition, the coupled ratchets display symmetry-breaking, saddle-nodes and bubbles of bifurcations. Chaotic behavior is characterized by using the Lyapunov exponent spectrum; while a perusal of the phase space projected in the Poincaré cross section confirms some of the striking features.

DOI: 10.1103/PhysRevE.72.056213 PACS number(s): 05.45.Pq, 02.30.Oz, 05.45.Xt

I. INTRODUCTION

Coupled nonlinear systems possess a rich catalog of potentially useful dynamical behaviors including bifurcations, chaos, and synchronization. They are central to the understanding of a wide variety of extended systems, e.g., a line of lattice oscillations or coupled plasma wave modes. A system of two oscillators could make a Hopf bifurcation to a second incommensurate frequency and follow a quasiperiodic route to chaos, in addition to period doubling and intermittency. Such routes to chaos was first observed by Ruelle and Takens [1]. Synchronization phenomena in coupled or driven nonlinear oscillators are of fundamental importance and have been extensively investigated both theoretically and experimentally in the context of many specific problems arising in laser dynamics, electronic circuits, secure communications, and time series analysis [2], to mention a few. For a more detailed and comprehensive description on different types of synchronization likely to be observed in two or more coupled systems, the reader can refer to the book of Pikovsky *et al.* [3]. In a recent study, we examined the synchronization of both unidirectionally [4] and bidirectionally [5] coupled deterministic ratchets that exhibits intermittent chaos. In [4,5], it was shown that the transition to the synchronous regime is characterized by an interior crises transition of the attractor in the phase space. Specifically, two analytic tests based on the Fujisaka and Yamada approach [6,7] and that of Gauthier and Bienfang [8] were employed to verify the stability of the synchronous state in reference [4].

A clear understanding of coupled oscillator systems requires a study of the full spectrum of the operating regimes, including the nonsynchronous state [9]. It has been reported that a group of interacting chaotic units that exhibits synchronization show some bifurcation cascades from disorder to partial and global order when varying the coupling strength [10]. Ding and Yang [11] showed the existence of intermingled basins in coupled Duffing oscillators that exhibit synchronized chaos and conjectured that intermingled basins can be easily realized in the context of coupled oscillators and synchronized chaos. Extensive bifurcation analysis of two coupled periodically driven Duffing oscillators was done by Kozlowski *et al.* [12]. They showed that the global pattern of bifurcation curves in parameter space consists of repeated subpatterns similar to the superstructure observed for single, periodically driven, strictly dissipative oscillators. This study was recently extended to two coupled periodically driven double-well Duffing oscillators by Kenfack [13]. The results revealed a striking departure from the single-well Duffing oscillators studied by Kozlowski *et al.* [12].

The literature is abundant with studies on coupled oscillator systems. At this point, we wish to refer the reader to

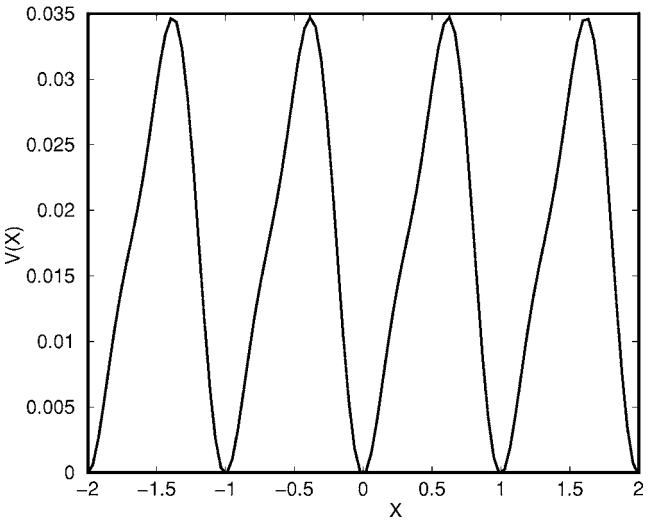

FIG. 1. The dimensionless ratchet potential.

*Corresponding author. Electronic address: kenfack@mpipks-dresden.mpg.de

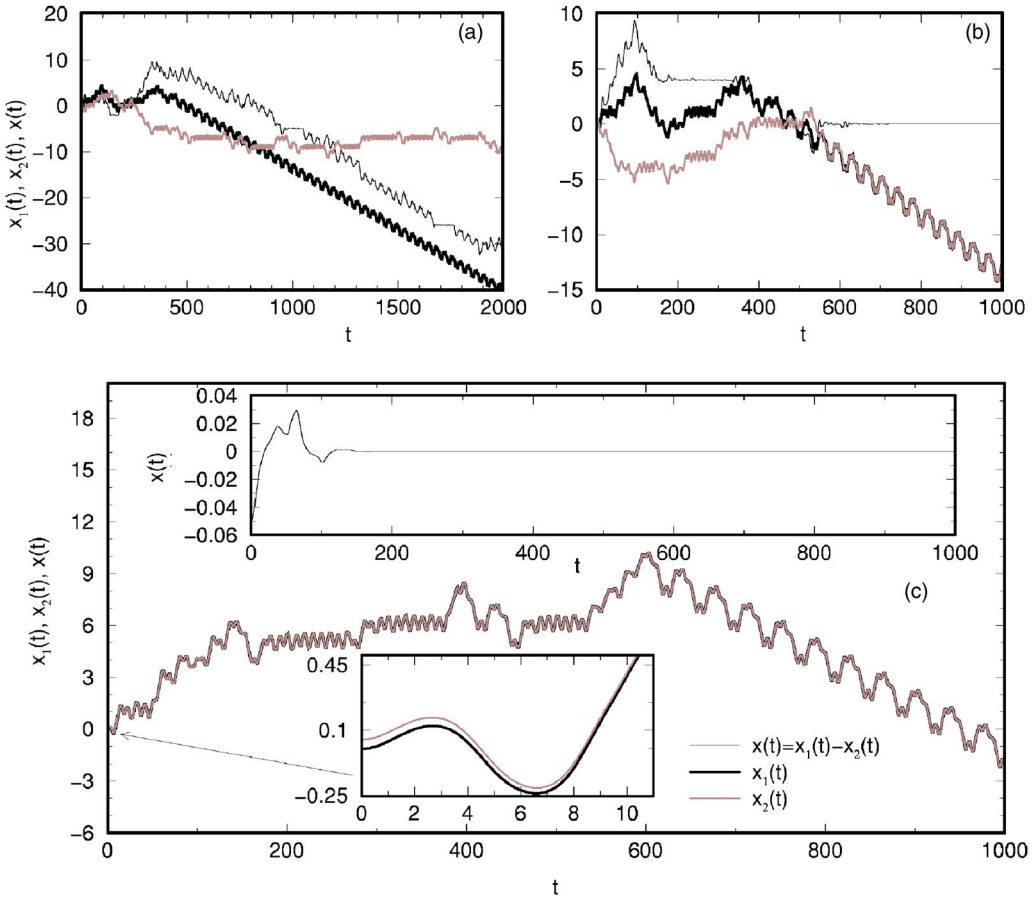

FIG. 2. (Color online) Synchronization dynamics showing the time dependent quantities $x_1(t)$, $x_2(t)$, $x(t)=x_1(t)-x_2(t)$ for $b=0.1$, $a=0.08092844$, $\omega=0.67$ and for different values of the coupling strength c: (a) $c=0.01$, no synchronization, (b) $c=0.9$, synchronization after a long transcient time $t\approx 450$, and (c) $c=0.95$, synchronization after a short transcient time $t\approx 8$.

some other recent studies that are related to the subject of this work [14–21]. Motivated by this series of studies, we aim in this paper to explore some dynamical features hitherto not fully explored in the coupled ratchets with emphasies on the bifurcation structures preceeding the synchronous regime. The rest of the paper is organized as follows: Section II describes the equations of motion of the chaotic ratchet model and comments on the synchronization behavior of the coupled system that is of interest in this study. In Sec. III, we carry out a linear stability analysis of the system projected on the Poincaré map, while in Sec. IV, numerical results of bifurcations are presented. Chaotic behavior is characterized in Sec. V. The paper is concluded in Sec. VI.

II. THE CHAOTIC RATCHET MODEL

Let us consider the one-dimensional problem of a particle driven by a periodic time-dependent external force under the influence of an asymmetric potential of the ratchet type [22–26]. The time average of the external force is zero. In the absence of stochastic noise, the dynamics is exclusively deterministic. We are thus concerned with a rocked deterministic ratchet satisfying the following dimensionless inertial dynamics:

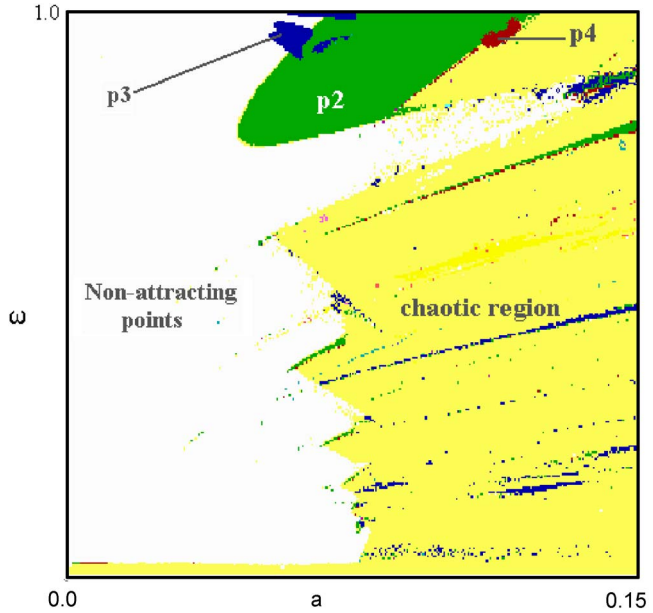

FIG. 3. (Color online) Two parameter phase diagram in the $(a$-$\omega)$ plane, for $b=0.1$ and $c=0.5$. Regions of period-2 (p2) in green, period-3 (p3) in blue, period-4 (p4) in red, chaos in yellow, and nonattraction in white can be identified.

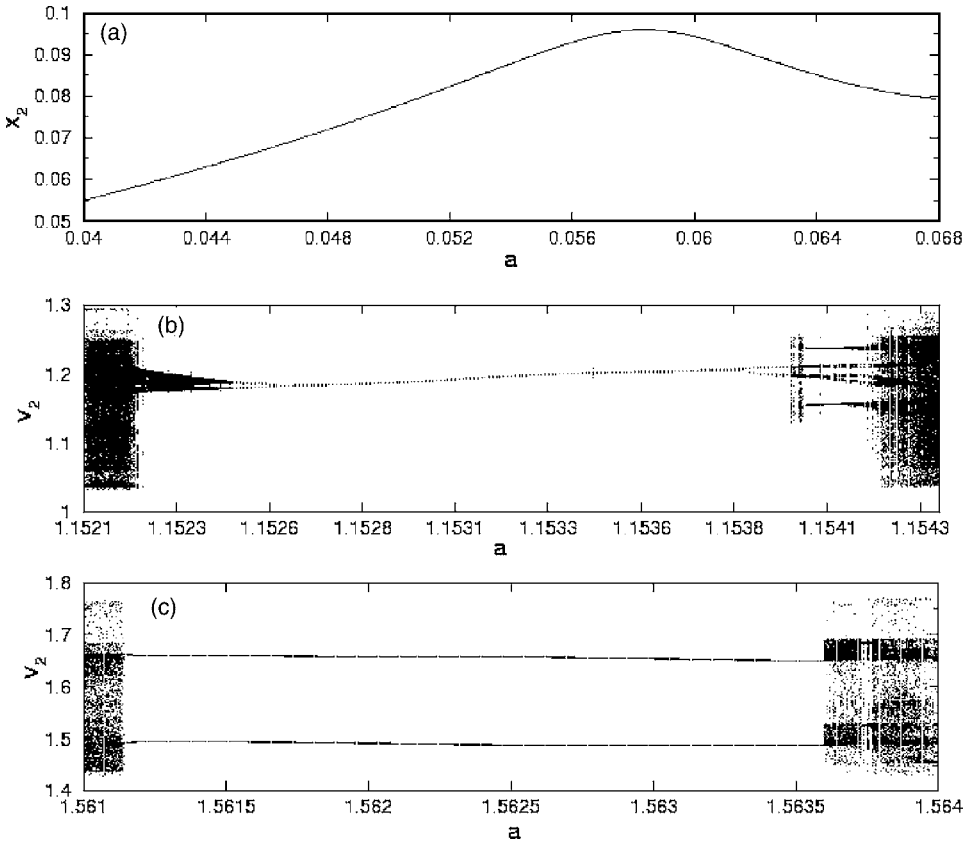

FIG. 4. Bifurcation diagrams for $\omega=0.3$, $b=0.1$, and $c=0.5$ showing (a) a resonance near $a=0.0559$, (b) a period-1, and (c) a large windows of period-2, both sandwiched in the chaotic regions.

$$\ddot{x} + b\dot{x} + \frac{dV(x)}{dx} = a\cos(\omega t) \tag{1}$$

in the asymmetric ratchet potential $V(x)$, where a and b are the forcing strength and the damping parameter, respectively. The period associated to the frequency ω_0 of the linear motion around the minima of the ratchet potential has been used as the natural time unit to scale time. The above formulation implies that all quantities used here are dimensionless. Thus the dimensionless potential $V(x)$ is given by

$$V(x) = C - \frac{1}{4\pi^2\delta}[\sin 2\pi(x-x_0) + 0.25\sin 4\pi(x-x_0)], \tag{2}$$

with constants $C \simeq 0.0173$ and $\delta \simeq 1.6$. The potential $V(x)$ is shifted by a value x_0 in order to place its minimum at the origin (see Fig. 1). Notice that this asymmetric potential is periodic and has an infinite number of potential wells.

The extended phase space in which the dynamic is taking place is three-dimensional, since we are dealing with an inhomogeneous differential equation with an explicit time dependence. We can rewrite Eq. (1) in autonomous form as a three-dimensional dynamical system described by the coordinates:

$$\dot{x} = y,$$

$$\dot{y} = a\cos\theta - by - \frac{dV(x)}{dx},$$

$$\dot{\theta} = \omega. \tag{3}$$

Since Eq. (3) is nonlinear, its solutions allow the possibility of periodic and chaotic orbits. For the purpose of this study, we consider a system of two identical unidirectionally coupled chaotic ratchets governed by [4]

$$\ddot{x}_1 + b\dot{x}_1 + \frac{dV(x_1)}{dx_1} = a\cos(\omega t), \tag{4}$$

$$\ddot{x}_2 + b\dot{x}_2 + \frac{dV(x_2)}{dx_2} = a\cos(\omega t) + c(\dot{x}_1 - \dot{x}_2), \tag{5}$$

where c is the coupling parameter. For $a=0.08092844$, $b=0.1$ and $\omega=0.67$, systems (4) and (5) exhibit complete synchronization when $0.89 \leqslant c \leqslant 1.05$. Complete synchronization, or simply sychronization, means suppression of differences in coupled identical systems [3]. To describe this phenomenon in our chaotic model, we examine the behavior of the time dependent quantity $x(t)=x_1(t)-x_2(t)$. The synchronization is achieved as $x(t)$ tends to be constant. In such a situation, the state of the two systems coincide and vary chaotically in time. The synchronization dynamics for different values of the coupling strength c is shown in Fig. 2. It turns out that for a very weak coupling $c=0.01<0.89$ (a), the two chaotic ratchets do not synchronize. However, for a much larger coupling strength, a complete synchronization is reached after a long transcient time ($t \approx 450$) for $c=0.9$ (b) and for a very short transcient time ($t \approx 8$) for $c=0.95$ (c); see also insets. Prior to the onset of synchronization, the

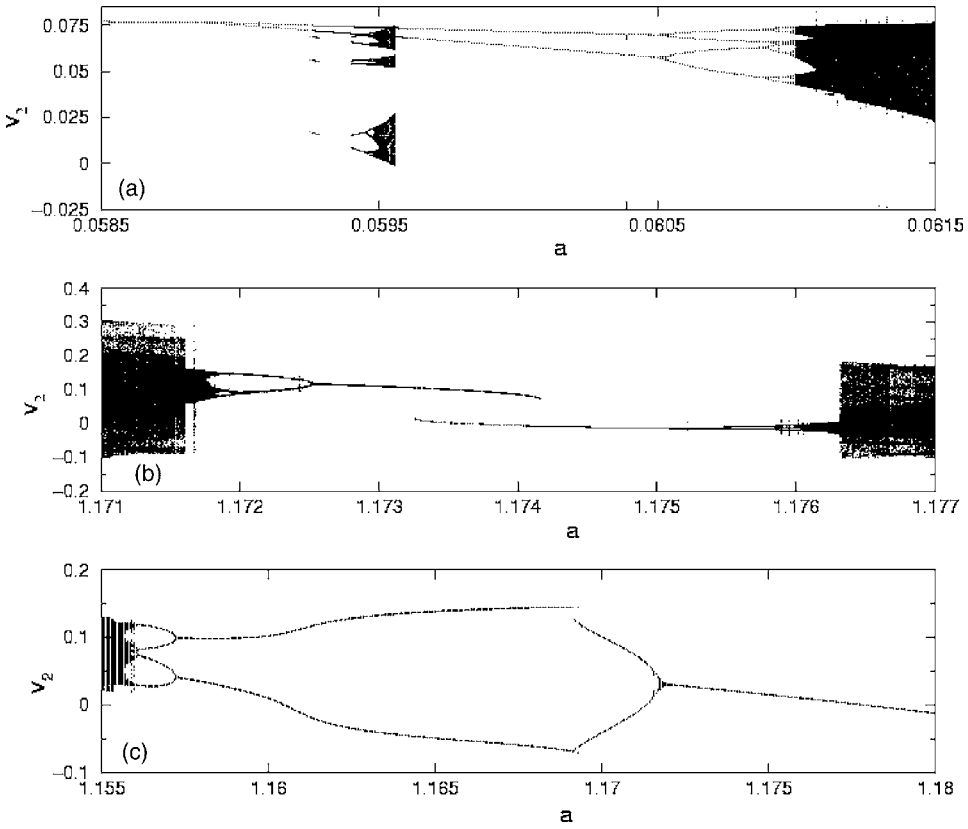

FIG. 5. Bifurcation diagrams for $b=0.1$ and $c=0.5$ and for the driving frequencies (a) $\omega=0.4$, (b) $\omega=0.5$, and (c) $\omega=0.75$ showing clearly the occurence of *sn*, *sb*, reversed *pd* and *pd* route to chaos.

strange attractor undergoes a crises transition during which it is gradually destroyed and as the synchronization regime is approached, the attractor is again rebuilt [4]. In a very recent work, Kostur *et al.* [27] studied systems (4) and (5) with time-delay coupling schemes, thus corresponding to a master-slave model. They found that the slave ratchet, under the time-delay coupling can respond the same way as the master will respond in the future, thereby anticipating the nonlinear directed transport. To obtain approximate visualization of the attractors and their bifurcations we follow the procedure described in [12,13]. That is, we investigate the dynamics in the Poincaré sections denoted by Σ.

III. STABILITY ANALYSIS

To begin with, let us consider the basic mathematical principle underlying some expected topological structure of the coupled ratchets. Here we carry out a stability analysis of the coupled system (4) and (5) which can be written equivalently as

$$\dot{x}_1 = v_1,$$

$$\dot{v}_1 = a\cos(2\pi\theta) - bv_1 + \frac{1}{4\pi\delta}[2\cos 2\pi(x_1 - x_0) + \cos 4\pi(x_1 - x_0)],$$

$$\dot{x}_2 = v_2,$$

$$\dot{v}_2 = a\cos(2\pi\theta) - bv_2 + \frac{1}{4\pi\delta}[2\cos 2\pi(x_2 - x_0) + \cos 4\pi(x_2 - x_0)] + c(v_1 - v_2),$$

$$\dot{\theta} = \frac{\omega}{2\pi}. \tag{6}$$

We denote by $(x_1, v_1, x_2, v_2, \theta)$ any element of the state space $\mathrm{IR}^4 \times S^1$, where S^1 is the unit circle containing θ. For better visualizing attractors and their bifurcations diagrams, the dynamics is explored in the Poincaré cross section defined by

$$\sum = \{(x_1, v_1, x_2, v_2, \theta = \theta_0) \epsilon \mathrm{IR}^4 \times S^1; \quad \theta_0 = \mathrm{const}\}.$$

The constant θ_0 determines the location of the Poincaré cross section on which coordinates of attractors $X(x_1, v_1, x_2, v_2)$ are expressed. By employing the linear perturbation method which consists of considering the solution $X(x_1, v_1, x_2, v_2)$ as a superposition of a very small perturbation $Y(\delta x_1, \delta v_1, \delta x_2, \delta v_2)$ to the steady state $V_0(x_{10}, v_{10}, x_{20}, v_{20})$, that is $X = V_0 + Y$, we obtain the matrix variational equation

$$\dot{Y} = DG(V_0)Y \tag{7}$$

where $DG(V_0)$ is the 4×4 Jacobian matrix

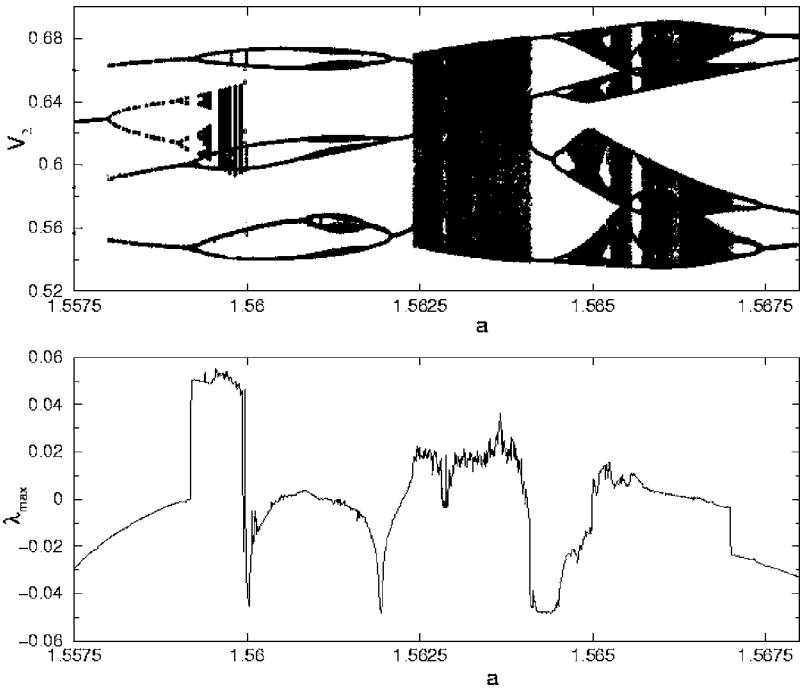

FIG. 6. (a) Bifurcation diagram for $c=0.5$, $b=0.1$, $\omega=0.5$ and (b) the corresponding Lyapunov spectrum in the Poincaré map.

$$DG(V_0)=\begin{pmatrix} 0 & 1 & 0 & 0 \\ \alpha & -b & 0 & 0 \\ 0 & 0 & 0 & 1 \\ 0 & c & \beta & -(b+c) \end{pmatrix} \tag{8}$$

describing the vector field along the solution Y and V_0 being an equilibrium point or steady state with $\alpha=-2/\delta[1+3\pi(x_{10}-x_0)]$; $\beta=-2/\delta[1+3\pi(x_{20}-x_0)]$. The solution of Eq. (7) after one period T of the oscillations is given by

$$Y(T)=Y(0)\exp(DG(V_0)T), \tag{9}$$

where $DG(V_0)$ represents the time-independent stability matrix of a periodic orbit connecting arbitrary infinitesimal variations in the initial conditions $Y_0=Y(0)$ with corresponding change in $Y(T)$. The real parts of the roots of the characteristic equation $\det(DG(V_0)-I\lambda)=0$, given by

$$\lambda^4+A_3\lambda^3+A_2\lambda^2+A_1\lambda+A_0=0, \tag{10}$$

determine the stability of the periodic motion, with $A_3=2b+c$, $A_2=b(b+c)-(\alpha+\beta)$, $A_1=-b(\beta+\alpha)+\alpha c$ and $A_0=\alpha\beta$. Here $\lambda=(\lambda_j)$ represent the eigenvalues of $DG(V_0)$. If one assumes $x_0\approx x_{10}\approx x_{20}$, as in our numerical experiment, then $\alpha=\beta=-2/\delta$. In general, complex eigenvalues occur in complex conjugate pairs. Let us consider α_k, β_k as the real and the imaginary parts of λ_k, respectively ($\lambda_k=\alpha_k+i\beta_k$). If λ_k is real, the eigenvalues are simply the rate of contraction ($\alpha_k<0$) or expansion ($\alpha_k>0$) near the steady state. If λ_k is complex, besides the role played by α_k, the imaginary part β_k contributes to the frequency rotation of the spiral. The eigenvalues of the Poincaré map may thus be written as

$$\sigma_k=\exp(\alpha_k T)[\cos(\beta_k T)+i\sin(\beta_k T)]. \tag{11}$$

It turns out from Eq. (11) that if $\alpha_k<0$ for all λ_k, then all sufficiently small perturbations tend torward zero as $t\to\infty$ and the steady state [node (n), saddle-node (sn), spiral (sp)] is stable. If $\alpha_k>0$ for all λ_k, then any small perturbation grows with time and the steady state (n,sn,sp) is unstable. In addition if there exist m and l such that $\alpha_m<0$ and $\alpha_l>0$, the equilibrium state is unstable and is called a saddle. Having recourse to the above analysis it follows that saddle-node, $sn(\lambda_k=+1)$, period-doubling, $pd(\lambda_k=-1)$, Hopf ($\beta_k\neq 0$, with $\alpha_k<0$), and symmetry-breaking (sb) bifurcations are expected to occur in the coupled ratchets. Similar bifurcational scenarios have been found in periodically driven coupled single [12] and double [13] well Duffing oscillators.

IV. BIFURCATION DIAGRAMS

In order to investigate the dependence of the system on a single control parameter (in this case, the amplitude a of the driving function), several bifurcation diagrams have been computed, some of which have been chosen to illustrate the general structure of the system. Each bifurcation diagram shows the projection of the attractors in the Poincaré section onto the x_2 or the v_2 coordinates versus the control parameter. We employ this technique in our numerical exploration using the period $T=2\pi/\omega$ of oscillation as the stroboscopic time; with the standard fourth- order Runge Kutta algorithm.

We begin with a general overview of the behavior of the two coupled systems by displaying regions of existence of different periodic and chaotic orbits in a two parameter phase diagram which is plotted in the (a-ω) plane at fixed values of $b=0.1$ and $c=0.5$ (Fig. 3). This diagram is obtained using the software dynamics [28]. Different regions of periodic orbits of period-2 (green), period-3 (blue), period-4 (red), as well as chaotic orbits (yellow) are clearly visible. Besides the periodic and the chaotic orbits, there also exist nonattracting points (white) for which the orbits diverge; any trajectory starting in such a white area is expected to leave it for ever as

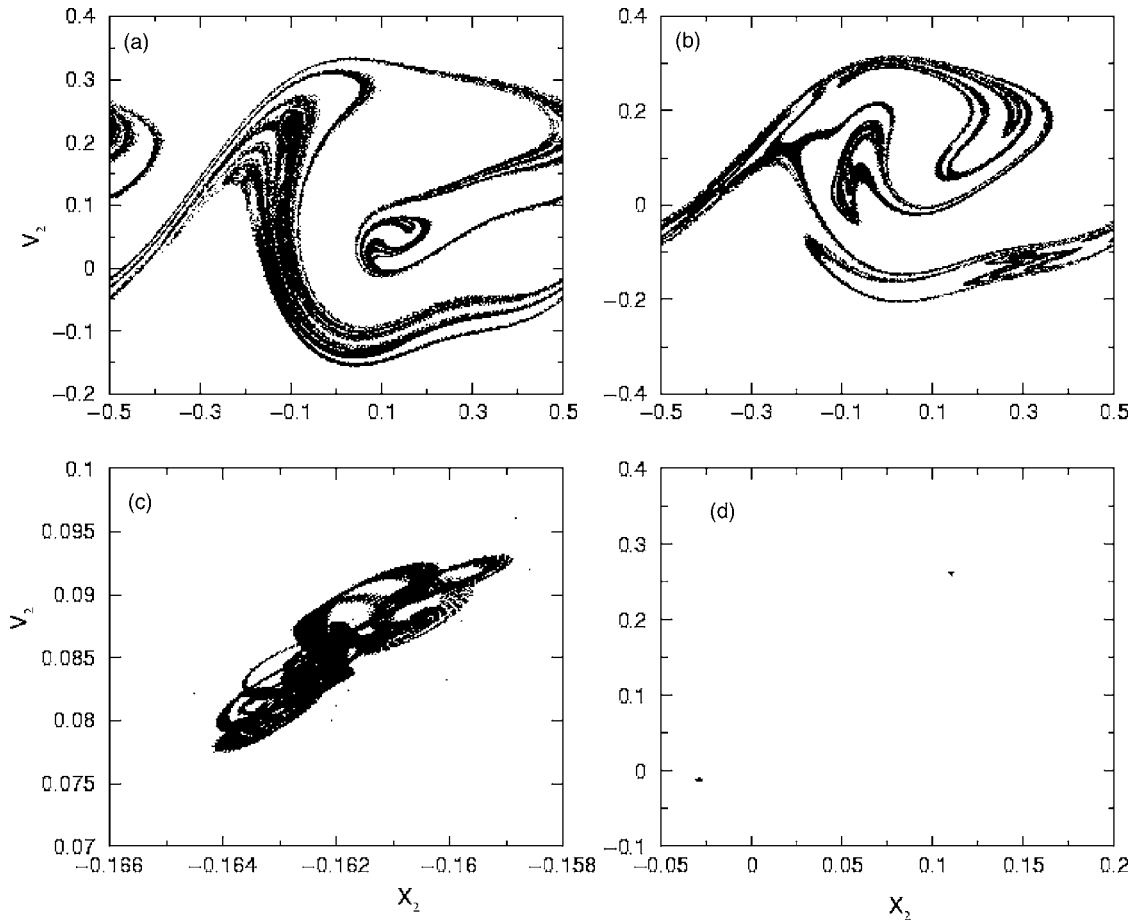

FIG. 7. Typical attractors for parameters taken from Fig. 3, with fixed values of $a=0.08092844$, $b=0.1$, and $c=0.5$. Shown are chaotic attractors (a) for $\omega=0.4$, (b) for $\omega=0.5$, (c) for $\omega=0.75$, and (d) a quasiperiodic attractor of period-2 for $\omega=0.8$.

time goes by and the variables take very large numbers (infinity). The present phase diagram is not providing any information about the synchronized states but rather about the different periodic-chaotic transitions that may occur in the systems. We found that for a given value of (a,ω), both ratchets are in the same regime though not having identical time series $[x(t)\neq 0$, nonsynchronous regime].

In all examples that follow, we fixed $b=0.1$ and $c=0.5$; the values for which the coupled ratchets do not synchronize. In Fig. 4 we show bifurcation diagrams for a comparatively small driving frequency of $\omega=0.3$. Different bifurcation sequences occur as the driving amplitude a is varied. For instance, in Fig. 4(a), there is a resonance near $a=0.0559$ while a period-1 attractor emerges in Fig. 4(b) from chaos, through a reversed period-doubling (*pd*) and subsequently follows the familiar *pd* route to chaos. For a much larger amplitude of the driving force, a large period-2 is suddenly created at around $a=1.5612$ from a chaotic region [see Fig. 4(c)]. This period-2 attractor is finally annihilated in a crisis event around $a=1.5638$ leading to a sudden chaotic state (transcient chaotic state). After this chaotic state we find bubbles of bifurcation dominating periodic windows [further, see Fig. 6(a) as a prototype]. When the driving frequency ω is increased, saddle-node (*sn*), symmetry breaking (*sb*) bifurcations, quasiperiodicity as well as period-doubling (*pd*) cascade predominate. For instance in Fig. 5(a), there is occurence of (*sn*) in the vicinity of $a=0.05925$ where coexisting attractors show up and a *pd* cascade, at around $a=0.06075$, leading to chaos for $\omega=0.4$. Moreover *sb* and *sn* resulting from a reversed *pd* are clearly visible in Fig. 5, (b) for $\omega=0.5$ and (c) for $\omega=0.75$. Similar routes identified in this transport model have also been found in the coupled Duffing model [12,13].

To complete our bifurcation study, we proceed to investigate large values of the driving frequency ($\omega>\omega_c=0.8$) and different ranges of a. Here we find that the majority of the earlier observed bifurcation scenarios are also repeated except that for large a, typically greater than the critical value $a_c=1.17$, periodic attractors dominate. Fingerprints of such behavior can readily be observed in Fig. 5(c) for $\omega=0.75$, where a period-1 attractor is created via a *sb* bifurcation.

V. CHARACTERIZING CHAOS

To better validate the results obtained above, it is necessary to compute the Lyapunov exponent which is well known as a powerful indicator of chaos in dynamical systems. Also it will be interesting to visualize the attractors in a more concrete space—the Poincaré cross sections.

The set of Lyapunov exponents λ_k can be obtained from linear stability analysis. In this approximation, all solutions

are of the form $\exp(\lambda_k t)$, $k=1,2,\ldots,M$. The maximum Lyapunov exponent λ_{max} is defined as

$$\lambda_{max} = \lim_{\tau\to+\infty} \frac{1}{\tau} \ln(\|L(\tau)\|), \tag{12}$$

where $\|L(\tau)\| = (\delta x_1^2 + \delta v_1^2 + \delta x_2^2 + \delta v_2^2)^{1/2}$ is obtained in the Poincaré cross section by solving numerically the variational equation (7) simultaneously with the systems (4) and (5). A positive Lyapunov exponent is a signature of chaos while zero and negative values of the exponent is an indication of a marginally stable or quasiperiodic orbit and periodic orbit, respectively. In Fig. 6(b), a spectrum of the λ_{max}, corresponding to the bifurcation diagram of Fig. 6(a) obtained for $\omega=0.5$, is displayed. Regions of chaotic and periodic solutions are well characterized. Various bifurcation scenarios can be found including *sn*, *sb*, quasiperiodic region, *pd* cascade leading to chaos, and bubbles of bifurcation.

Finally in Fig. 7, we visualize the attractors in the Poincaré cross sections for a fixed valued of the driving force $a=0.080928844$ and for several values of the driving frequency ω taken from Fig. 3. We find that as ω increases, the chaotic attractor shrinks [see Fig. 7, (a) for $\omega=0.4$, (b) for $\omega=0.5$, and (c) for $\omega=0.75$]. As a consequence, the attractor size gets enlarged as ω decreases. Essentially, this phenomenon has been attributed to the collision of the attractor with a periodic orbit in the exterior of its basin and is thus referred to as boundary crises [29]. For larger ω values, quasiperiodic and periodic attractors were found to dominate. As an example, Fig. 7(d) shows a quasiperiodic attractor of period-2 for $\omega=\omega_c=0.8$.

VI. CONCLUSIONS

In summary, we have investigated the dynamics of unidirectionally coupled deterministic ratchets and have shown varieties of bifurcation sequences including the quasiperiodic route to chaos. Using the standard method of linear stability analysis, we have examined the stability of the steady state solution of the system leading to different types of bifurcations likely to occur in the neigborhood of the synchronized region. For a given driving frequency, the bifurcations depend strongly on the values of the driving amplitude a and are generally complicated. Besides quasiperiodicity, the familiar period-doubling and crisis route to chaos were also observed. In addition, the coupled ratchets exhibit symmetry-breaking bifurcations, resonance, saddle-node, and bubbles of bifurcations. Using the Lyapunov exponent spectrum, we characterized chaos in this system. A perusal of the Poincaré cross sections revealed boundary crises in which the size of chaotic attractor is suddenly enlarged as the driving frequency is gradually decreased for a fixed driving amplitude. Although this system presents a very chaotic structure, it remains nevertheless ordered as the driving frequency becomes large, thereby providing critical parameters for a chaotic transport of particles.

ACKNOWLEDGMENTS

U.E.V gratefully acknowledges Professor Jose L. Mateos of the Instituto de Fisica, Universidad Nacional Autonoma de Mexico, Mexico, for supplying relevant literatures and very useful discussions. A.K. gratefully acknowledges the Reimar Lüst grant and the financial support of the Alexander von Humboldt (AvH) Foundation/Bonn-Germany, under the grant of Research fellowship No IV.4-KAM 1068533 STP. We are grateful to Dr. E. Arevalo for a careful reading of the manuscript.

[1] D. Ruelle and F. Takens, Commun. Math. Phys. **20**, 167 (1971).
[2] Z. Zhang, X. Wag, and M. C. Cross, Phys. Rev. E **65**, 056211 (2002).
[3] A. Pikovsky, M. Rosenblum, and J. Kurths, *Synchronization: A Universal Concept In Nonlinear Sciences* (Cambridge University Press, Cambridge, England, 2001).
[4] U. E. Vincent, A. N. Njah, O. Akinlade, and A. R. T. Solarin, Chaos **14**, 1018 (2004).
[5] U. E. Vincent, A. N. Njah, O. Akinlade, and A. R. T. Solarin, Physica A (to be published).
[6] H. Fujisaka and T. Yamada, Prog. Theor. Phys. **69**, 32 (1983).
[7] T. Yamada and H. Fujisaka, Prog. Theor. Phys. **70**, 1240 (1983).
[8] D. J. Gauthier and J. C. Bienfang, Phys. Rev. Lett. **77**, 1751 (1996).
[9] R. J. Ram, R. Sporer, A. R. Blank, and R. A. York, IEEE Trans. Microwave Theory Tech. **48**, 1909 (2000).
[10] G. Hu, Y. Zhang, H. A. Cerdeira, and S. Chen, Phys. Rev. Lett. **85**, 3377 (2000).
[11] M. Ding and W. Yang, Phys. Rev. E **54**, 2489 (1996).
[12] J. Kozlowski, U. Parlitz, and W. Lauterborn, Phys. Rev. E **51**, 1861 (1995).
[13] A. Kenfack, Chaos, Solitons Fractals **15**, 205 (2003).
[14] S. Wirkus and R. Rand, Nonlinear Dyn. **30**, 205 (2002).
[15] P. Woafo, J. C. Chedjou, and H. B. Fotsin, Phys. Rev. E **54**, 5929 (1996).
[16] G. L. Baker, J. A. Blackburn, and H. J. T. Smith, Phys. Rev. Lett. **81**, 554 (1998).
[17] Y. Chen, G. Rangarajan, and M. Ding, Phys. Rev. E **67**, 026209 (2003).
[18] T. Hikihara, K. Torii, and Y. Ueda, Phys. Lett. A **281**, 155 (2001).
[19] H. J. T. Smith, J. A. Blackburn, and G. L. Baker, Int. J. Bifurcation Chaos Appl. Sci. Eng. **13**, 7 (2003).
[20] A. F. Va Kakis and R. Rand, Int. J. Non-Linear Mech. **39**, 1079 (2004).
[21] S. P. Raj, S. Rajaskar, and K. Murali, Phys. Lett. A **264**, 283

(1999).
[22] P. Jung, J. G. Kissner, and P. Hanggi, Phys. Rev. Lett. **76**, 3436 (1996).
[23] J. L. Mateos, Phys. Rev. Lett. **84**, 258 (2000).
[24] J. L. Mateos, Physica D **168-169**, 205 (2002).
[25] J. L. Mateos, Physica A **325**, 92 (2003).
[26] J. L. Mateos, Commun. Nonlinear Sci. Numer. Simul. **8**, 253 (2003).
[27] M. Kostur, P. Hänggi, P. Talkner, and J. L. Mateos, Phys. Rev. E **72**, 036210 (2005).
[28] H. E. Nusse and J. A. Yorke, *Dynamics: Numerical Exploration* (Springer-Verlag, Berlin, 1998).
[29] E. Ott, *Chaos in Nonlinear Dynamical Systems* (*Cambridge University Press*, Cambridge, England, 2002).